

Density functional investigation of the geometric and electronic structure of ethylene adsorbed on Si(001)

U. Birkenheuer,^{a)} U. Gutdeutsch, and N. Rösch

Lehrstuhl für Theoretische Chemie, Technische Universität München, 85747 Garching, Germany

A. Fink, S. Gokhale, D. Menzel, P. Trischberger, and W. Widdra

Physik-Department E20, Technische Universität München, 85747 Garching, Germany

(Received 2 January 1998; accepted 13 March 1998)

A detailed first-principles density functional analysis of the geometric and electronic properties of ethylene adsorbed on the dimer reconstructed Si(001)-(2×1) surface is presented. This theoretical study was carried out in close reference to a recent angle-resolved photoemission spectroscopy investigation of the same adsorption system. Adsorbate weighted Kohn-Sham one-particle spectra are calculated and compared to the band structure derived from the angle-resolved photoemission spectra. In addition, the symmetry character of the concomitant Bloch waves is determined to yield information which can directly be related to the results of a dipole selection rule analysis of the corresponding photoemission signals. Total energy minimization of a model slab reveals a distortion of the adsorption complex at saturation coverage to local C_2 symmetry involving an 11° rotation of the ethylene molecule around the surface normal and a 27° twist of the methylene groups around the C-C axis. This finding is confirmed by a comparison of the calculated band dispersions with those found in the angle-resolved ultraviolet photoelectron spectroscopy (ARUPS) experiments. The driving forces for the distortion of the adsorption complex can be traced to direct Pauli repulsion between the hydrogen atoms of neighboring ethylene molecules and to a bonding overlap contribution from the ethylene $1b_{2g}$ -derived orbitals of the adlayer. © 1998 American Institute of Physics. [S0021-9606(98)01523-2]

I. INTRODUCTION

Motivated by technologically important processes such as chemical vapor deposition, diamond film growth, and formation of silicon carbide on crystalline silicon, and accompanied by a more general interest in the reactivity of nonpassivated silicon surfaces, the interaction of hydrocarbons with silicon surfaces has been studied quite extensively in the past. However, it was only a decade ago that adsorption of unsaturated hydrocarbons on the well-characterized dimer-reconstructed Si(001)-(2×1) surface was investigated for the first time (Ref. 1 for C_2H_2 , Ref. 2 for C_2H_4). Many experimental studies on acetylene³⁻⁷ and ethylene^{3,7-13} adsorption followed. Except for an infrared spectroscopy investigation on the reaction paths of the two stereoisomers of 1,2-dideuteroethylene,¹³ all these experimental studies focused on the thermal and vibrational properties of the adsorption complexes. It was soon accepted that both, acetylene and ethylene, are di- σ bound to one of the Si-Si dimers of the reconstructed Si(001) surface. Two structure models have been proposed: a dimerized structure,^{1,2} where the hydrocarbon binds to the dangling bonds of a surface Si-Si dimer without breaking the dimer bond [Fig. 1(a)], and a dimer-cleaved structure,^{4-6,9} where the adsorbate is inserted in the Si dimer bond, leading to a di-radical structure with one unsaturated dangling bond left on each silicon atom [Fig.

1(b)]. Chemically intuitive arguments such as the necessity of saturating dangling bonds or the energetic disadvantage of strongly distorted tetrahedral bonding angles were put forward in the discussion about these two models, until in 1993 for the first time direct experimental information about the nature of the adsorption complex was obtained by atomic hydrogen coadsorption experiments.^{7,10-12} It was demonstrated that in the low-exposure regime atomic hydrogen very efficiently binds to a hydrocarbon precovered Si(001) surface and that, as far as thermal and vibrational properties are concerned, the initial adsorption complex is not altered significantly by the presence of the coadsorbate. These findings were taken as experimental evidence for a dimer-cleaved structure of ethylene¹⁰⁻¹² on Si(001)-(2×1) with dangling bonds ready to bind the subsequent hydrogen. However, hydrogen *initiated* Si-Si dimer cleavage, first proposed by Fisher *et al.*¹⁴ based on first-principles slab model calculations, and very recently confirmed theoretically by Pan *et al.*,¹⁵ must be regarded as a serious alternative bonding mechanism which complicates the interpretation of the coadsorption experiments.

In the meantime, quite a few theoretical investigations have been devoted to the adsorption of hydrocarbons on Si(001)-(2×1): some based on semiempirical methods,¹⁶⁻²² but also, more recently, on first-principles density functional (DF) calculations for both acetylene^{14,22-24} and ethylene.^{14,15,23} The energetic preference between the two controversial structure models was not analyzed explicitly in all of them, but if done,^{14-18,22,24} the dimerized structure was

^{a)} Author to whom correspondence should be addressed. Electronic mail: birken@theochem.tu-muenchen.de; fax: ++49+89 289-13622.

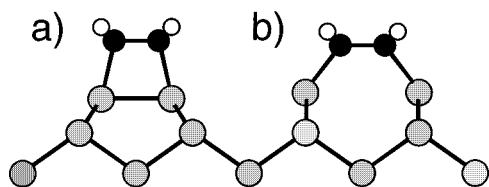


FIG. 1. Schematic view of (a) the dimerized and (b) the dimer-cleaved structure models for C_2H_2 and C_2H_4 adsorbed on the Si(001)-(2 \times 1) surface.

always found to be more stable with energy differences in the order of 1.0–1.5 eV for C_2H_2 and 0.9–1.5 eV for C_2H_4 . (Note the Erratum¹⁷ to Ref. 16.) Only once, some evidence for an energetically more favored dimer-cleaved structure was encountered:¹⁹ Within a mixed quantum potential plus classical force field molecular dynamics investigation of the sticking probability of acetylene on Si(001), flipping between dimerized and dimer-cleaved structures of the adsorbate was observed which finally died out in a dimer-cleaved and thus di-radical equilibrium configuration. In that investigation the semiempirical AM1 method²⁵ was employed for the quantum region. However, it was demonstrated more recently²⁶ that compared to other semiempirical methods the AM1 parametrization performs particularly poorly on organo-silicon radicals. Thus, calculations clearly favor the dimerized structure for the adsorption complexes $C_2H_2/Si(001)$ and $C_2H_4/Si(001)$, even if one takes into account that spin-restricted density functional theory might have some difficulties in properly describing homosymmetric di-radical structures (like the dimer-cleaved one).

Finally, direct STM (scanning tunneling microscopy) images of ethylene adsorbed on Si(001), as recently recorded by Mayne *et al.*,^{27,28} did not provide any further information about the fate of the Si–Si dimer bond.

In striking contrast to the large amount of experimental data available on the thermal and vibrational properties of hydrocarbons on silicon, investigations on the *electronic* structure of these adsorption systems are rare. No such study has ever been performed for acetylene or ethylene on Si(001), and besides our recent ARUPS (angle-resolved ultra-violet photoelectron spectroscopy) investigation of benzene on Si(001)-(2 \times 1),²⁹ we are aware of only three further examinations of the electronic structure of hydrocarbons on silicon: an UPS study (not angularly resolved) of acetylene and ethylene on Si(111),³⁰ and two similar studies on the adsorption of benzene on Si(111).^{31,32} Furthermore, none of the previous density functional slab model calculations for $C_2H_4/Si(001)$ ^{14,15} actually reported the one-particle band structure of the adsorption system.

The present theoretical investigation therefore focuses on the electronic structure and the lateral interactions of ethylene adsorbed on Si(001)-(2 \times 1). In a very recent angle-resolved photoemission study of C_2H_4 on single-domain Si(001)-(2 \times 1) using synchrotron radiation, the electronic structure of the adsorption system has been investigated in detail.^{33,34} It was shown that some of the adsorbate-derived states feature one-dimensional dispersion.³³ Furthermore, evidence for a symmetry reduction of the adsorbate complex from C_{2v} to C_2 was found.³⁴ Here we report on the accom-

panying density functional investigation of that adsorption system. We start by a more general discussion on the changes in the electronic structure of hydrocarbons due to adsorption on a silicon surface. Then the results of the first-principles slab model calculations on the geometrical and electronic structure of the adsorption system are presented. Finally, the calculated Kohn-Sham one-particle spectra will be compared to the experimental data and both the reduction of the local symmetry of the adsorption complex and its relation to the observed lateral interadsorbate interaction will be analyzed and discussed in detail.

II. COMPUTATIONAL DETAILS

Except for some preliminary cluster studies on the geometrical and electronic structure of ethylene on Si(001) which were carried out on a semiempirical level by means of the modified neglect of differential overlap method³⁵ MNDO/*d* as implemented in the SIBIQ program³⁶ (employing a parametrization for Si which includes *d* functions²⁶), all theoretical results presented here have been obtained with the WIEN95 code,³⁷ a FLAPW (full-potential linearized augmented plane-wave) realization of the Kohn-Sham approach to density functional theory. Gradient-corrected exchange correlation functionals³⁸ have been used throughout. The adsorption system is simulated by a six-layer Si(001) slab with ethylene being adsorbed on both sides of the slab. Adsorbates and surface Si dimers were allowed to relax while the Si atoms of the innermost four layers were fixed at their bulk positions, using the experimental lattice constant of 5.43 Å.³⁹ The thickness of the vacuum region separating the repeated slabs corresponds to 7.5 layers of Si(001), which results in interslab hydrogen-hydrogen distances (of the adsorbed ethylene molecules) of about 5.8 Å. Test calculations have shown that in this geometrical setup no noticeable energy dispersion occurs along the [001] direction in any of the occupied states of the adsorption system. The muffin-tin radii were chosen rather small (1.9 for Si, 1.2 for C, and 0.75 au for H) to avoid overlapping spheres during the geometry optimization. The plane-wave cutoff for the wave functions was set to 17.4 Ry, that of the potential representation had to be chosen *much* higher, 196 Ry, to ensure analytical forces consistent with the potential energy surface (see also remarks in Ref. 40). The surface Brillouin-zone was sampled by 32 *k*-points which correspond to 16 (C_2) or 8 (C_{2v}) irreducible *k*-points depending on the symmetry of the adsorption complex.

III. RESULTS

A. Qualitative considerations on adsorbate photoemission

It is common practice in the interpretation of photoemission spectra of molecules adsorbed at surfaces to start by directly relating the adsorbate induced photoemission features to the occupied orbitals of the isolated, gas-phase adsorbate (e.g., the UPS studies on hydrocarbons on Si(111)^{30–32}). This procedure relies on the fact that very often the orbitals of the adsorbate are not altered very significantly by the presence of the substrate.

In the case of a silicon substrate, the situation is much too complicated for this procedure to be sensible. First, one has to consider that the interaction of nonpassivated silicon (001) surfaces with unsaturated (or aromatic) hydrocarbons can result in the formation of strong covalent Si–C bonds. If so, the structure and chemical configuration of the adsorbate may be substantially distorted, and thus it might be more appropriate to use the corresponding hydrogen addition product as reference. For benzene adsorbed on Si(001), for example, it was recently found²⁹ that the photoemission spectrum of condensed cyclohexadiene bears much more similarity to the spectrum of the adsorption complex than that of condensed benzene. However, also for states which do not form new strong covalent bonds upon chemisorption, significant changes of their orbitals can occur, if their energies do not fall into a band gap of the substrate (eventually k_{\parallel} -resolved), and provided the coupling to Bloch states of the substrate is not suppressed otherwise, e.g., by orbital symmetry. For unsaturated or aromatic hydrocarbons interacting with transition metals, the energies of most of the occupied states of the adsorbate are well below the quite narrow d band of the substrate. This allows direct correlation of gas-phase orbitals with those in the adsorption complex as has been demonstrated in many investigations (e.g., Refs. 41 and 42, and references therein). However, for silicon the width of the valence band amounts to more than 12 eV (e.g., Ref. 43), and thus Si substrate states are available with energies low enough to couple with most of the hydrocarbon states. Depending on both the energetic position and the particular shape and orientation of the nodal planes of the orbitals involved, new orbitals of the adsorption complex are formed. Some of these adsorbate orbitals may happen to exhibit only minor admixtures of substrate states (the so-called resonances); other adsorbate orbitals may couple quite strongly to the substrate states and become delocalized spatially as well as energetically. The former type of orbitals will give rise to pronounced signals in the photoemission spectra, whereas emission from the latter orbitals may be hard to detect within the background intensity.

In order to specialize this discussion to the adsorption system $C_2H_4/Si(001)$, an orbital correlation diagram derived from semiempirical model cluster calculations is shown in Fig. 2. On the left-hand side the one-particle spectra of ethylene in the gas phase (exhibiting D_{2h} symmetry) and in the geometry of the adsorption complex, respectively, are given. The coupling of the ethylene orbitals $3a_g$ and $1b_{2u}$ due to chemisorption induced symmetry reduction to C_{2v} is the most pronounced feature here. On the right-hand side, the electronic structure of the substrate is shown schematically: the isolated dangling bond states of a single surface dimer in the band gap, as well as the valence and conduction bands (represented as boxes). Upon adsorption, the C $2s$ related low-lying valence orbitals $2a_g$ and $2b_{1u}$ remain separated from the silicon valence band. All other orbitals spread more or less distinctively as indicated by the shaded areas in Fig. 2. Neither the Si dangling bond states nor the ethylene highest occupied molecular orbital (HOMO) and lowest unoccupied molecular orbital (LUMO), $1b_{2u}$ and $1b_{3g}$, are any more discernible in the electronic structure of the adsorption

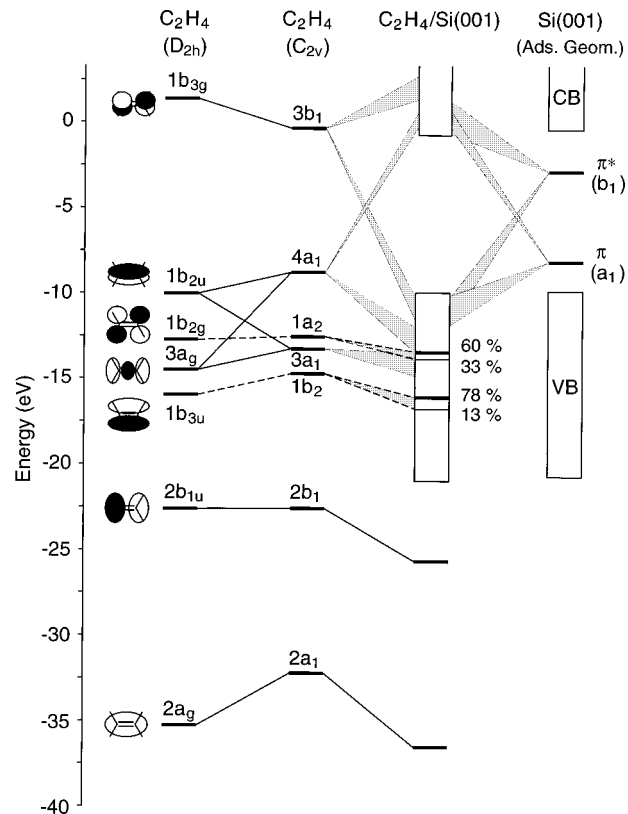


FIG. 2. Orbital correlation diagram for adsorption of ethylene on a Si_9H_{12} model cluster of the Si(001)-(2 \times 1) surface as resulting from MNDO/ d calculations. On the left-hand side the energy levels of gas-phase ethylene (D_{2h} symmetry) and of ethylene in the geometry of the adsorption complex (C_{2v} symmetry) are shown together with sketches of the corresponding molecular orbitals. On the right-hand side the energy levels of the substrate cluster are indicated schematically. In the central panel the energy levels of the adsorption system are shown. States which are even with respect to the vertical mirror plane along the C–C bond are connected by solid lines, odd states are connected by dashed lines. A 7% cutoff has been employed to identify the orbital correlations indicated by the shaded areas.

complex, a fact which indicates the formation of new (covalent) Si–C bonds. Of the altogether nine localized orbitals that are involved in the adsorbate-substrate interaction, after chemisorption only two remain strongly localized at the adsorbate: an a_2 symmetric feature at about -13 eV with 60% ethylene $1b_{2g}$ admixture, and a b_2 symmetric feature roughly 3 eV below the a_2 symmetric one with almost 80% admixture of the ethylene orbital $1b_{3u}$. These two ethylene orbitals are precisely those which contain a vertical nodal plane through the C–C bond and the underlying Si–Si dimer bond. Obviously this particular arrangement and the accompanying reduced direct orbital overlap very efficiently suppress coupling to the substrate states which might be feasible from an energy point of view. In principle, a similar effect may be expected for the $3a_g$ orbital because of its nodal structure. However, closer inspection reveals that this orbital is so much distorted by “upward” bending of the hydrogen atoms (see Fig. 1) that a direct σ overlap toward the silicon dimer atoms becomes possible.

B. Structural optimization

All calculations for ethylene on Si(001) performed so far which allowed full relaxation of the adsorption

TABLE I. Comparison of calculated equilibrium geometries of various models used to represent the adsorption system $C_2H_4/Si(001)$. H and H' denote the two nonequivalent hydrogen atoms of the C_2 symmetric structure (see Fig. 3). Bond lengths are given in Å, angles in degrees.

Method Model	DF ^a (GGA) slab	DF ^a (GGA) slab	MNDO/ <i>d</i> ^a (semi.) cluster	DF ^b (LDA) slab ^f	DF ^c (LDA) slab	MINDO ^d (semi.) slab	ASED ^e (semi.) cluster
Symmetry	C_2 ^g	C_{2v} ^g	C_{2v}	C_{2v}	C_{2v}	C_{2v}	C_{2v} ^g
$d(CH)$	1.103	1.101	1.12		1.13		1.092 ^h
$d(CH')$	1.102						
$d(CC)$	1.496	1.498	1.57	1.53	1.52	1.494	1.59 ^h
$d(SiC)$	2.006	2.007	1.93	1.95	1.93	1.813 ⁱ	2.01
$d(SiSi)$	2.393	2.391	2.32		2.33	2.389	
$\angle(HCH')$	106.9	106.8	107	106.7	105.3		108
$\angle(CCH)$	115.5	113.8	112	113	113.3		110
$\angle(CCH')$	112.7						
$\angle(CCSi)$	102.3	102.8	101		102.1	104.3	97
$\alpha(CC)^j$	11.4						

^aThis work.

^bReference 14.

^cReference 15.

^dReference 17.

^eReference 21.

^fUsing a (4×4) overlayer to model a quarter of the saturation coverage.

^gEnergy minimization restricted to specified symmetry.

^hCalculated using $d_{\text{theo}} - d_{\text{exp}}$ of Ref. 21 and d_{exp} of Ref. 49.

ⁱCalculated using $d(CC)$, $d(SiSi)$, and $z(C) - z(Si) = 1.757 \text{ \AA}$ of Ref. 17.

^jRotation angle of the C–C bond round the surface normal.

complex^{14–16,24} led to C_{2v} symmetric equilibrium configurations. This was also found here in preliminary semiempirical test calculations using a C_2H_4/Si_9H_{12} model cluster: a unique C_{2v} -symmetric minimal total energy configuration with an uncleaved Si–Si dimer was obtained, irrespective of whether a symmetric or nonsymmetric starting configuration was used, or whether the optimization was started with a dimer-cleaved or a dimerized structure (see Fig. 1). Details of this structure are given in Table I (col. 4). In a first step, our density functional slab calculations for ethylene chemisorbed on $Si(001)-(2 \times 1)$ have therefore been carried out preassuming local C_{2v} symmetry of the adsorption complex. According to the experimental data available,^{2,3,7,10–12} a saturation coverage of half a monolayer (one adsorbate for each Si dimer) is adopted, though a (2×1) low-energy electron diffraction (LEED) pattern not necessarily implies that each surface Si–Si dimer participates in the chemisorption. For example, a (2×1) LEED pattern is also observed for the adsorption system $C_6H_6/Si(001)-(2 \times 1)$ which definitely only exhibits a quarter monolayer coverage at saturation.⁴⁴ In line with previous DF investigations,^{14,15,24} a dimerized equilibrium structure was found (Table I, col. 3). Except for the C–C bond length which is calculated longer by 0.07 Å in the semiempirical cluster approach than in the DF slab calculations, the internal structure of the adsorbed ethylene predicted by the two methods is rather similar. The structure of the substrate, however, differs significantly: both the Si–Si dimer bond length as well as the Si–C bond distance are underestimated by the semiempirical method by 0.07–0.08 Å. Similar observations about the limitations of the MNDO/*d* approach concerning the structure of bulk ma-

terials and atoms in the direct vicinity of surfaces have been made in a recent investigation on the adsorption of benzene on $Si(001)-(2 \times 1)$.⁴⁴

In Table I we compare the structural parameters reported in previous theoretical studies on the adsorption of ethylene on $Si(001)-(2 \times 1)$ to those of the present work. Most of these values lie within the range spanned by our DF slab and MNDO/*d* cluster model calculations. However, two major deviations are worth noting. The Si–C bond length is predicted far too short by the semiempirical MINDO (modified intermediate neglect of differential overlap) approach,¹⁷ 0.19 Å with respect to the DF results, and an amazingly small C–C–Si bond angle of 97° results from the semiempirical atom superposition and electron delocalization (ASED) cluster calculations.²¹ The latter deviation is most probably due to the unrelaxed Si–Si dimer bond length of 2.23 Å used in the ASED study.²¹ We are unable to offer a rationalization for the extremely short Si–C distance calculated by the MINDO investigation.¹⁷

On the other hand, as already mentioned, our angle-resolved UPS data provide quite distinct evidence for a reduced C_2 symmetry of the adsorption complex.³⁴ The density functional model slab calculations have therefore been repeated under less stringent symmetry constraints, and indeed, a local minimum was found 0.023 eV lower in energy than the metastable C_{2v} symmetric configuration (see Table I, col. 2). The C–C axis of the adsorbate is rotated by 11.4° around the surface normal resulting in a Si–C–C–Si dihedral angle of 13° (see Fig. 3). This rotation is accompanied by a further 14° twist of the two methylene groups, as can be seen in the Newman projection of the adsorption complex along

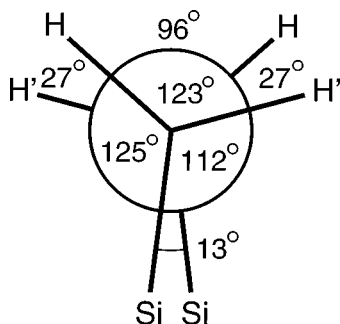


FIG. 3. Newman projection along the ethylene C–C axis for the distorted C_2 symmetric structure of the adsorption complex resulting from the DF slab calculations. H and H' denote nonequivalent hydrogen atoms.

the C–C axis shown in Fig. 3. The remaining structural parameters, especially the Si–Si, Si–C, and C–C bond lengths are essentially the same for both configurations (Table I). The largest deviations ($\pm 1.5^\circ$) occur in the C–C–H bond angles. A rationalization of this distortion will be proposed in Sec. IV.

C. The electronic structure

We now turn to a discussion of the electronic structure of the adsorption complex. We start by giving a brief summary of the experimental results.^{33,34} In Fig. 4 two angle-resolved spectra for a photoemission polar angle of 45° along the $[110]$ and the $[1\bar{1}0]$ high symmetry directions are depicted for a photon energy of 50 eV. The data (described in detail elsewhere³⁴) exhibit seven ethylene-derived peaks in the valence band region. Six of them are clearly discernible in Fig. 4, whereas the $3a_g$ state is resolvable for a few emission angles only. A detailed analysis of spectra at different photon energies in the range of 26 to 70 eV, and different experimental conditions regarding light polarization and angle of incidence as well as emission angles, reveal that the local symmetry of the adsorbate complex is reduced from

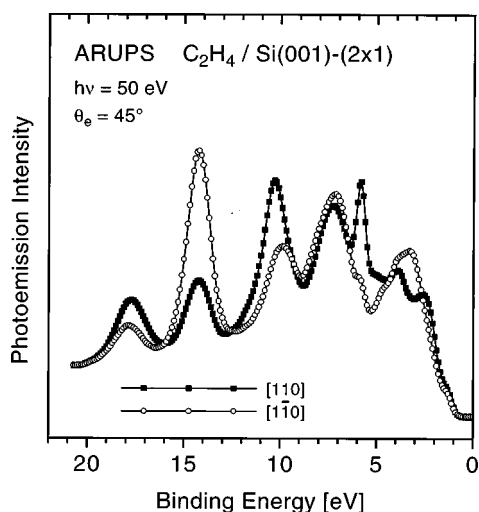


FIG. 4. Angle-resolved UPS spectra for ethylene saturation on single-domain Si(001)-(2 \times 1) collected for a polar angle of 45° along the $[110]$ and $[1\bar{1}0]$ azimuth. Synchrotron radiation with a photon energy of 50 eV and an angle of incidence of 45° was used.

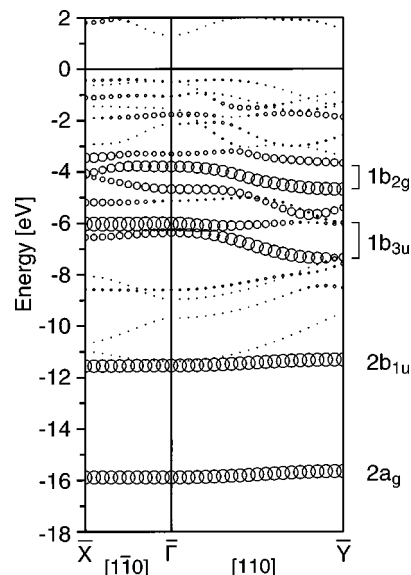


FIG. 5. Adsorbate population weighted band structure of the model slab for the adsorption system $C_2H_4/Si(001)$ in the C_2 symmetric equilibrium configuration. Only electronic states which are even with respect to the glide plane of the system are shown (see text). The orbital energies are given relative to the Fermi level. The diameters of the circles are proportional to the adsorbate population.

C_{2v} to C_2 .³⁴ Furthermore, two ethylene-derived states, $1b_{3u}$ and $1b_{2g}$, exhibit significant dispersion of 1.2 and 0.8 eV, respectively, along the $[110]$ direction and no dispersion perpendicular to that direction.³³ The periodicity of the 1D dispersing bands corresponds quite well to a (2 \times 1) overlayer, confirming the half monolayer coverage model used here for $C_2H_4/Si(001)$.

To rationalize these findings and to assist in the assignment of the photoemission signals, the band structure and the symmetry of the concomitant Bloch states found in the DF slab calculations will be analyzed in the following. Comparison of measured valence ionization energies and electron affinities with Kohn-Sham one-particle energies has been applied successfully in many investigations; see, for example, the studies on the adsorption of hydrocarbons on transition metal surfaces^{42,45} or on the chemisorption of benzene on Si(001).^{29,44} Within this approach, surface sensitivity is generally achieved by projecting the electronic structure on the adsorbate (and occasionally on the first substrate surface layers as well). In the present investigation the adsorbate population is determined by a subdivision of the repeated slab in real space. Planes parallel to the surface which intersect the Si–C bonds in the ratio of the muffin-tin radii involved are used for that purpose. Because of the rather small radii adopted (see Sec. II) these planes do not intersect any muffin-tin sphere of the repeated slab model, a circumstance which simplifies the calculation of the populations tremendously. All integrals required for the population analysis could be evaluated analytically.⁴⁶

In Fig. 5 the band structure of the C_2 symmetric equilibrium structure of the adsorption system is shown. Due to the “sandwich” model employed, two more or less degenerate bands are expected for each localized surface feature. However, in order to facilitate the interpretation, only even

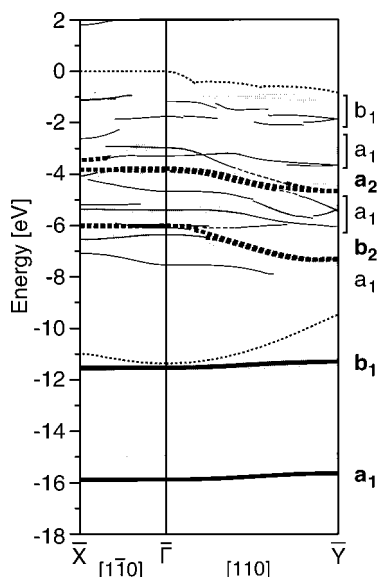


FIG. 6. Comparison of the adsorbate related features of the experimental band structure of $C_2H_4/Si(001)$ (Ref. 34) (shown schematically in gray) with the calculated bands of the C_2 symmetric adsorption complex which exhibit at least 25% adsorbate admixtures. The experimental band structure is shifted to align the $2b_{1u}$ band with the calculated one at -11.6 eV. Upper and lower bounds of the silicon valence band of the finite slab model are indicated by dotted lines. Bands with more than 80% adsorbate population are marked in bold; bands related to the ethylene orbitals $1b_{3u}$ and $1b_{2g}$ are marked by dashed lines.

eigenstates with respect to the glide plane symmetry of the six-layered slab model are displayed in Fig. 5. Here, even and odd eigenstates ψ_{nk}^\pm refer to the phase factor $\pm \exp(ikt)$ resulting from the glide plane operation $\{\sigma_{xy}|t\}$. The selection itself is carried out by means of symmetry projectors.⁴⁶ The amount of adsorbate population for each band is indicated by the diameter of the circles in Fig. 5.

Four adsorbate-dominated band complexes are discernible in the calculated band structure of ethylene on $Si(001)-(2 \times 1)$. The two isolated bands at -15.9 and -11.5 eV which exhibit 93% and 86%–91% adsorbate population, respectively, are the surface states of the adsorption system which are derived from the ethylene orbitals $2a_g$ and $2b_{1u}$. The third adsorbate-dominated feature is given by the split band running from -6.0 eV at \bar{X} down to -7.4 eV at \bar{Y} . A detailed symmetry analysis and inspection of the Bloch waves reveals that an accidental avoided crossing occurs close to the $\bar{\Gamma}$ point and that in fact the split band is entirely related to an ethylene $1b_{3u}$ -derived state over the entire Brillouin zone. This assignment is confirmed by the band structure of the odd eigenstates where only a single continuous adsorbate-dominated band is found in the energy range between -7.4 and -6.0 eV (see Fig. 6). Finally, the fourth adsorbate-dominated feature between -4.7 and -3.4 eV turns out to be exclusively associated with an ethylene $1b_{2g}$ -derived state, although again accidental degeneracy due to avoided crossings occurs (e.g., at the \bar{X} point in Fig. 5). Two of these adsorbate-derived bands exhibit significant dispersion along the dimer rows, in full agreement with the experimental findings.³³

All band complexes discussed so far are related to well-

localized surface states, as can be judged from the minor splitting of the bands associated with the corresponding even and odd Bloch waves. For the low-lying C $2s$ -derived $2a_g$ and $2b_{1u}$ states the splittings amount only to 0.003 and 0.022 eV, respectively, and thus are not discernible at all in Fig. 6 where all bands, even as well as odd ones, with an adsorbate population of more than 25% are displayed. Similar observations hold for the $1b_{3u}$ - and the $1b_{2g}$ -derived bands (Fig. 6, bold dashed lines). Except for the avoided crossings, the bands of the even and odd linear combinations of the associated surface states are essentially degenerate. However, there also exist bands with less dominant adsorbate admixtures. Energetically, they are located in the upper half of the silicon valence band, between -7 and -1 eV (Fig. 6). The corresponding Bloch waves are far less localized, and it is not possible to identify degenerate even-odd pairs. Despite their adsorbate admixture, none of these states can be uniquely associated with either ethylene, surface Si dimer, or Si–C bond orbitals. These findings completely confirm the qualitative picture for the electronic structure of ethylene adsorbed on silicon which was derived from the semiempirical orbital correlation diagram in Sec. III A.

Yet one has to keep in mind that only adsorbate populations have been considered so far. However, localized subsurface features such as the back-bond states in a clean $Si(001)-(2 \times 1)$ surface can also give rise to prominent photoemission signals.⁴⁷ Such states are not well represented by the adsorbate population-weighted band structure shown in Fig. 5. Thus there may very well be some bands which yield much stronger electron emission than indicated by their ethylene admixtures. Population analyses focusing on the surface Si–Si dimers have therefore been performed as well (not shown). However, we were not able to identify any strongly localized Si–Si dimer or Si–C bond states. This was expected to some extent since back-bond states, for example, are known to extend over several silicon layers.⁴³ Nevertheless, some indications for such silicon related features can be found: The adsorbate admixture to the split band complex between -2 and -1 eV, discernible in Fig. 5, are accompanied by an enhanced Si $3p_z$ population. Analysis of the expectation values of properly chosen symmetry projectors⁴⁶ reveals that the concomitant Bloch waves are essentially antisymmetric with respect to the mirror plane intersecting the Si–Si dimer of the adsorption complex. Thus, there is some evidence that the band complex discussed here is related to a moderately localized subsurface feature including an antisymmetric linear combination of the two newly formed Si–C bonds. In a similar way, the symmetric counterpart was identified between -3.5 and -3.0 eV, although it is even harder to discern in the expectation values.

IV. DISCUSSION

Both the experimental band structure derived from the ARUPS data, as well as the band structure calculated for the slab model, exhibit bands with significant dispersion. The most pronounced dispersion values, 1.4 and 0.9 eV, respectively, are calculated for the $1b_{3u}$ - and $1b_{2g}$ -derived bands (see Table II). Very similar dispersions ($1b_{3u}$:1.3 eV, $1b_{2g}$:0.6 eV) are found for an unsupported monolayer of

TABLE II. Dispersion of the ethylene $1b_{3u}$ - and $1b_{2g}$ -derived bands in various models of the adsorption system $C_2H_4/Si(001)$. An average value is given where accidental splitting occurs in the calculated band structure (at most ± 0.13 eV, see text).

System	Symmetry	Dispersion (eV)	
		$1b_{3u}$ (b_2)	$1b_{2g}$ (a_2)
$C_2H_4/Si(001)$	C_{2v}	1.3	1.5
$C_2H_4/Si(001)$	C_2	1.4	0.9
C_2H_4 monolayer	C_2	1.3	0.6
Experiment		1.2	0.8

ethylene molecules arranged as in the C_2 symmetric configuration of the adsorption system. We therefore conclude that the observed dispersion is mainly due to direct lateral "through space" interaction of the adsorbed molecules. This finding is in line with the strong localization of the Bloch waves involved, as can be seen in the wave function contour plots⁴⁶ shown in Fig. 7 for the $\bar{\Gamma}$ point. The wave function amplitude within the substrate (indicated by the skeleton in Fig. 7) is far too small to give rise to any significant substrate mediated contributions to the dispersion. On silicon surfaces the occurrence of such a direct, lateral "through space" interaction in hydrocarbon adsorption systems may be somewhat surprising in view of the generally rather strong localization of the adsorbate-substrate bonds compared to typical metal-adsorbate bonds. However, one has to consider that the intermolecular H-H distance of 2.07 Å which occurs in the C_2 symmetric adsorbate layer (see Fig. 7) is of the same order as the closest interneighbor H-H distances (2.03 Å)

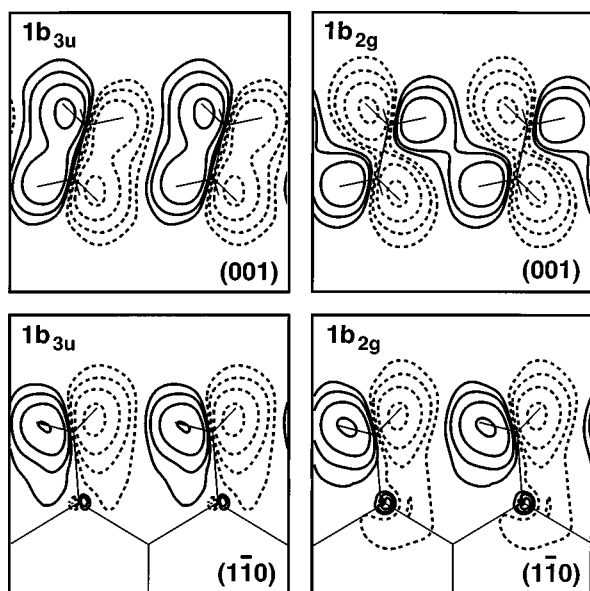


FIG. 7. The $1b_{3u}$ and $1b_{2g}$ -derived orbitals of the adsorption system $C_2H_4/Si(001)$ at the $\bar{\Gamma}$ point displayed in the (001) plane parallel to the surface as well as in the $(1\bar{1}0)$ plane perpendicular to the Si-Si dimers. Both planes are chosen such that they roughly intersect the C-H bonds of the adsorbate. The positions of the atoms are indicated by the (projected) bond skeletons. The values of the contour lines are ± 0.010 , ± 0.022 , ± 0.046 , and ± 0.100 au.

encountered in adsorption systems like $C_2H_4/Ni(110)$ where dispersion effects due to Pauli repulsion are well known.^{41,48}

There are several further observations which indicate that intermolecular hydrogen repulsion also occurs in the adsorption system $C_2H_4/Si(001)$. The most striking hint is that both the analysis of the selection rules of the ARUPS data as well as the total energy minimization of the model slab give evidence for a symmetry reduction of the adsorption complex from C_{2v} to C_2 . By this distortion the intermolecular H-H distances are enlarged by 0.16 Å with respect to the C_{2v} symmetric configuration. Apparently, interadsorbate repulsion between hydrogen atoms provides one of the driving forces for the symmetry reduction. This is confirmed by the overall twist of the methylene groups in the equilibrium structure which is about twice that required to solely follow the rotation induced twist of the Si-C bonds (see Fig. 3). However, a bonding orbital overlap effect is also involved in the symmetry reduction of the adsorption complex. In the C_{2v} reference geometry, the mutual interactions of both the $1b_{3u}$ - and the $1b_{2g}$ -derived Bloch waves are antibonding at the $\bar{\Gamma}$ point. Upon rotation of the adsorbate molecules around the surface normal, this antibonding overlap is reduced, and in the case of the a_2 symmetric $1b_{2g}$ -derived orbital even some bonding overlap between neighboring ethylene molecules is built up (see Fig. 7). This certainly contributes to the stabilization of the distorted adsorption complex (and also reduces the amount of dispersion, see below). Repulsive mutual interaction in the order of 0.25 eV/adsorbate pair has also been found in a recent repeated slab investigation of ethylene on $Si(001)-(2\times 1)$.¹⁴ There even is some independent experimental indication for such an interaction: A statistical analysis of STM images²⁸ taken for ethylene adsorbed at various coverages on a reconstructed $Si(001)$ surface revealed that the probability for nearest-neighbor ethylene adsorption is noticeably lower than expected for purely random adsorption.

No symmetry reduction was encountered in any of the previous first-principles calculations on ethylene adsorbed on $Si(001)$, neither at low coverage¹⁴ nor at saturation.¹⁵ Furthermore, with 0.023 eV the energetic preference of the distorted C_2 symmetric adsorption complex over the C_{2v} symmetric metastable configuration found in the present investigation is rather small. Thus one may speculate whether such a minute energy difference is significant or not. Note, however, that in the present investigation for the first time a generalized gradient-corrected energy functional has been used for the geometry optimization; all previous first-principles calculations^{14,15,23} relied on local density functionals in that point. As this difference is about the thermal energy for our experimental situation, we would expect that the distortion is dynamically averaged in the experiment.

There is another interesting detail which provides further independent evidence for symmetry reduction. Analysis of the band structure of the symmetric metastable configuration yields a dispersion for the $1b_{2g}$ band which is 0.2 eV larger than that of the $1b_{3u}$ band (Table II). For the distorted equilibrium structure the order in the size of the dispersion is reversed: with 0.9 eV, the $1b_{2g}$ band now exhibits less dispersion than the lower lying $1b_{3u}$ band. As already men-

tioned, this reduction in dispersion of the $1b_{2g}$ state is directly related to the particular nodal pattern of the concomitant Bloch waves (see Fig. 7) which allows bonding contributions once the ideal C_{2v} symmetry is broken. The experimentally determined band structures show dispersion widths of 1.2 and 0.8 eV for these states, respectively, in nice agreement with those calculated for the distorted structure (Table II). For a final comparison of the calculated band structure of the low-symmetry adsorption complex with the experimentally observed band structure, we refer to Fig. 6, where all bands of the model slab with an adsorbate population of more than 25% are shown. Although, strictly speaking, the model exhibits C_2 symmetry, it is worth trying to classify the individual bands according to the ideal C_{2v} symmetry of the adsorption complex. Inspection of the wave functions by means of symmetry projectors⁴⁶ onto the four irreducible representations of the point group C_{2v} reveals that almost everywhere the states can exclusively be attributed to one irreducible representation. As expected, the largest deviations occur for the $1b_{2g}$ band which drives the distortion. The assigned symmetry labels are given at the right-hand side of the band structure panel in Fig. 6. The experimental band structure and the symmetry characters deduced from a dipole selection rule analysis of the angular dependence of the photoemission signals³⁴ agree very well with the calculated data (see Fig. 6). The only experimental feature not discernible in the adsorbate weighted band structure is a b_1 symmetric state close to the Fermi level which has been attributed to substrate related features which emerge from the surface dimer states of the clean Si(001)-(2 × 1) surface.³⁴

V. SUMMARY

In the present first-principles slab model investigation, which has been carried out in close relation to a recent angle-resolved photoemission study,^{33,34} the structural and electronic properties of ethylene adsorbed on Si(001)-(2 × 1) have been analyzed. In line with previous density functional calculations,^{14,15} a dimerized structure is predicted for the adsorption complex. However, much more striking is the fact that a reduction of the local symmetry of the adsorption complex from C_{2v} to C_2 is found in this density functional investigation in which gradient-corrected exchange-correlation functionals have been consistently applied for both the forces entering the geometry optimization and the evaluation of the total energy.

In the resulting equilibrium configuration, the ethylene molecule is rotated by 11° around the surface normal and the two methylene groups of the adsorbate are twisted by 27° around the C–C axis (Fig. 3). The driving forces for this distortion are Pauli repulsion between the hydrogen atoms of neighboring adsorbates, on the one hand, and a covalentlike bonding overlap contribution from the ethylene $1b_{2g}$ -derived orbitals of the adsorption system, on the other hand (Fig. 7). According to a wave function analysis, the silicon substrate is not significantly involved in this interaction. Instead, quite substantial interadsorbate orbital overlap occurs in the adsorption system $C_2H_4/Si(001)$. The mutual orbital overlap between neighboring ethylene molecules also gives rise to

significant dispersion along the dimer rows in the adsorbate-dominated $1b_{3u}$ and $1b_{2g}$ bands, a finding which is in line with the experimental observations.³³ Moreover, only the dispersions calculated for the distorted C_2 symmetric structure (Table II) are in quantitative agreement with the corresponding values deduced from the ARUPS experiments.³³ This finding provides further independent evidence for the symmetry reduction.

The adsorbate-weighted band structure of the adsorption complex shown in Fig. 6 very nicely reproduces all adsorbate related photoemission features encountered in the accompanying ARUPS study.^{33,34} It further confirms the qualitative picture of the ethylene-silicon interaction which was derived from a semiempirical orbital correlation diagram of a C_2H_4/Si_9H_{12} model cluster (Fig. 2). The C $2s$ -derived $2a_g$ and $2b_{1u}$ orbitals of ethylene are far too low in energy to significantly interact with the silicon valence band. From the remaining valence orbitals only the $1b_{3u}$ and $1b_{2g}$ orbitals are maintained as strongly localized surface resonances upon chemisorption to the dimer-reconstructed Si(001) surface, an effect which could be traced to the vertical nodal plane along the C–C axis these orbitals contain. All other orbitals are absorbed in subsurface features; some of them are so delocalized that they may become quite hard to detect by photoemission spectroscopy. The important general conclusion therefore is that most of the features of the adsorbate bond are barely visible in the photoemission spectra. This is probably the reason why there is so much controversy about the adsorption system $C_2H_4/Si(001)$ -(2 × 1).

ACKNOWLEDGMENTS

We thank A. A. Voityuk for discussions on semiempirical methods and for providing his program SIBIQ. This work was supported by the Deutsche Forschungsgemeinschaft via SFB 338, the German BMBF via Grant No. WOA 625 05, and the Fonds der Chemischen Industrie.

¹M. Nishijima, J. Yoshinobu, H. Tsuda, and M. Onchi, *Surf. Sci.* **192**, 383 (1987).

²J. Yoshinobu, H. Tsuda, M. Onchi, and M. Nishijima, *J. Chem. Phys.* **87**, 7332 (1987).

³C. C. Cheng, R. M. Wallace, P. A. Taylor, W. J. Choyke, and J. T. Yates, Jr., *J. Appl. Phys.* **67**, 3693 (1990).

⁴T. J. Yates, Jr., *J. Phys.: Condens. Matter* **3**, S143 (1991).

⁵P. A. Taylor, R. M. Wallace, C. C. Cheng, W. H. Weinberg, M. J. Dresser, W. J. Choyke, and J. T. Yates, Jr., *J. Am. Chem. Soc.* **114**, 6754 (1992).

⁶C. Huang, W. Widdra, X. S. Wang, and W. H. Weinberg, *J. Vac. Sci. Technol. A* **11**, 2250 (1993).

⁷W. Widdra, C. Huang, S. I. Yi, and W. H. Weinberg, *J. Chem. Phys.* **105**, 5605 (1996).

⁸C. C. Cheng, W. J. Choyke, and J. T. Yates, Jr., *Surf. Sci.* **231**, 289 (1990).

⁹L. Clemen, R. M. Wallace, P. A. Taylor, M. J. Dresser, W. J. Choyke, W. H. Weinberg, and J. T. Yates, Jr., *Surf. Sci.* **268**, 205 (1992).

¹⁰W. Widdra, C. Huang, G. A. D. Briggs, and W. H. Weinberg, *J. Electron Spectrosc. Relat. Phenom.* **64/65**, 129 (1993).

¹¹C. Huang, W. Widdra, and W. H. Weinberg, *Surf. Sci.* **315**, L953 (1994).

¹²W. Widdra, C. Huang, and W. H. Weinberg, *Surf. Sci.* **329**, 295 (1995), Reply to Ref. 18.

¹³H. Liu and R. J. Hamers, *J. Am. Chem. Soc.* **119**, 7593 (1997).

¹⁴A. J. Fisher, P. E. Blöchl, and G. A. D. Briggs, *Surf. Sci.* **374**, 298 (1997).

¹⁵W. Pan, T. Zhu, and W. Yang, *J. Chem. Phys.* **107**, 3981 (1997).

¹⁶B. I. Craig and P. V. Smith, *Surf. Sci.* **276**, 174 (1992).

- ¹⁷B. I. Craig and P. V. Smith, *Surf. Sci.* **285**, 295 (1993), Erratum to Ref. 16.
- ¹⁸B. I. Craig, *Surf. Sci.* **329**, 293 (1995), Comment on Ref. 11.
- ¹⁹C. S. Carmer, B. Weiner, and M. Frenklach, *J. Chem. Phys.* **99**, 1356 (1993).
- ²⁰R. H. Zhou, P. L. Cao, and L. Q. Lee, *Phys. Rev. B* **47**, 10,601 (1993).
- ²¹P. L. Cao and R. H. Zhou, *J. Phys.: Condens. Matter* **5**, 2887 (1993).
- ²²Q. Liu and R. Hoffmann, *J. Am. Chem. Soc.* **117**, 4082 (1995).
- ²³K. Feng, Z. H. Liu, and Z. Lin, *Surf. Sci.* **329**, 77 (1995).
- ²⁴Y. Imamura, Y. Morikawa, T. Yamasaki, and H. Nakatsuji, *Surf. Sci.* **341**, L1091 (1995).
- ²⁵M. J. S. Dewar, E. G. Zoebisch, E. Healy, and J. J. Stewart, *J. Am. Chem. Soc.* **107**, 3902 (1985).
- ²⁶W. Thiel and A. A. Voityuk, *J. Mol. Struct.* **313**, 141 (1994).
- ²⁷A. J. Mayne, A. R. Avery, J. Knall, T. S. Jones, G. A. D. Briggs, and W. H. Weinberg, *Surf. Sci.* **284**, 247 (1993).
- ²⁸A. J. Mayne, C. M. Goringe, C. W. Smith, and G. A. D. Briggs, *Surf. Sci.* **348**, 209 (1996).
- ²⁹S. Gokhale, P. Trischberger, D. Menzel, W. Widdra, H. Dröge, H.-P. Steinrück, U. Birkenheuer, U. Gutdeutsch, and N. Rösch, *J. Chem. Phys.* **108**, 5554 (1998).
- ³⁰M. N. Piancastelli, R. Zanoni, D. W. Niles, and G. Margaritondo, *Solid State Commun.* **72**, 635 (1989).
- ³¹M. N. Piancastelli, M. K. Kelly, G. Margaritondo, J. Anderson, D. J. Frankel, and G. J. Lapeyre, *Appl. Surf. Sci.* **26**, 498 (1986).
- ³²M. N. Piancastelli, R. Zanoni, J. E. Bonnet, and K. Hricovini, *J. Electron Spectrosc. Relat. Phenom.* **68**, 383 (1994).
- ³³W. Widdra, A. Fink, S. Gokhale, P. Trischberger, D. Menzel, U. Birkenheuer, U. Gutdeutsch, and N. Rösch, *Phys. Rev. Lett.* (in press).
- ³⁴A. Fink, S. Gokhale, D. Menzel, P. Trischberger, W. Widdra, H. Koschel, U. Birkenheuer, U. Gutdeutsch, and N. Rösch (in preparation).
- ³⁵W. Thiel and A. A. Voityuk, *Int. J. Quantum Chem.* **44**, 807 (1992).
- ³⁶A. A. Voityuk, SIBIQ 2.4. A program for semiempirical calculations (1991).
- ³⁷P. Blaha, K.-H. Schwarz, P. Dufek, and R. Augustyn, WIEN95, Technical University of Vienna, 1995; P. Blaha, K.-H. Schwarz, P. Sorantin, and S. B. Trickey, *Comput. Phys. Commun.* **59**, 399 (1990).
- ³⁸J. P. Perdew, J. A. Chevary, S. H. Vosko, K. A. Jackson, M. R. Pederson, D. J. Singh, and C. Fiolhais, *Phys. Rev. B* **46**, 6671 (1992); J. P. Perdew and Y. Wang, *ibid.* **45**, 13,244 (1992).
- ³⁹N. W. Ashcroft and S. D. Mermin, *Solid State Physics* (Saunders, Philadelphia, 1976), Table 4.3.
- ⁴⁰B. Kohler, S. Wilke, M. Scheffler, E. Kouba, and C. Ambrosch-Draxl, *Comput. Phys. Commun.* **94**, 31 (1996).
- ⁴¹M. Weinelt, W. Huber, P. Zebisch, H.-P. Steinrück, B. Reichert, U. Birkenheuer, and N. Rösch, *Phys. Rev. B* **46**, 1675 (1992).
- ⁴²M. Weinelt, W. Huber, P. Zebisch, H.-P. Steinrück, P. Ulbricht, U. Birkenheuer, J. C. Boettger, and N. Rösch, *J. Chem. Phys.* **103**, 9709 (1995).
- ⁴³P. Krüger and J. Pollmann, *Phys. Rev. B* **38**, 10,578 (1988).
- ⁴⁴U. Birkenheuer, U. Gutdeutsch, and N. Rösch, *Surf. Sci.* (in press).
- ⁴⁵M. Weinelt, W. Huber, P. Zebisch, H.-P. Steinrück, M. Pabst, and N. Rösch, *Surf. Sci.* **271**, 539 (1992).
- ⁴⁶U. Birkenheuer, Extensions to the WIEN95 code (Ref. 37) 1997.
- ⁴⁷W. Widdra, S. Gokhale, P. Trischberger, and D. Menzel (unpublished).
- ⁴⁸U. Gutdeutsch, U. Birkenheuer, E. Bertel, J. Cramer, J. C. Boettger, and N. Rösch, *Surf. Sci.* **345**, 331 (1996).
- ⁴⁹J. L. Duncan, D. C. McKean, and P. D. Mallinson, *J. Mol. Spectrosc.* **45**, 221 (1973).